A Bio-Inspired Angle Dependent Damping Mechanism to Reduce Locomotive Variability in Passive Dynamic Bipedal Walkers

Kabir Knupp[1], Patrick D. McGuckian[1], Thrishantha Nanayakkara[2]

***Abstract*— This paper details the design and testing of a novel, bio-inspired, joint-angle dependent damping mechanism aiming to reduce the variability of bipedal passive dynamic locomotion.**

The non-deterministic nature of ground contact dynamics makes legged locomotion innately stochastic. Thus, to achieve reliable locomotion, researchers typically integrate complex control systems into their legged robots. However, biological walking systems may have a more elegant solution. Experiments have found that the angle-dependent damping profile of the knee joint reduces the variability of impact forces. This paper explores the potential of integrating this damping profile into robotic systems using a novel friction-based damping mechanism. The mechanism was tested on a 'toddler' style passive dynamic walker, by measuring its walking gait angle and step impact force as it walked down a ramp. 20 trials were conducted with the damper engaged, and 20 with it disengaged.

The results found that the mechanism reduced walking gait angle variability by 88% and helped the periodic behaviour of the machine's walking gait to converge. The damper also caused a 27% reduction in speed and an 8% increase in step frequency.

I. Introduction

Typical bipedal robotic systems use active sensor feedback and electric motors to accurately position limbs. Such systems have proven to be a reliable and adaptable method of robotic locomotion, however, they typically have an extremely high energy cost - with Honda's Azimo requiring roughly 16 times the energy to walk compared to the average human [1].

The efficiency of human locomotion can be accounted to our anatomy's innate 'passive dynamics'. Passive dynamics refers to the ability to convert input energy into useful actuation without active control - as demonstrated in passive dynamic walkers. First presented by McGeer in 1989, passive dynamic walkers convert their inputted energy into locomotion [2]. Initial systems used gravity as their energy source, allowing them to walk down slopes, however, subsequent systems have replaced this with a powered energy source, allowing them to walk on flat or inclined surfaces [1]. These powered passive dynamic systems have been demonstrated to have a similar energy efficiency to human locomotion.

However, like all legged locomotive systems, passive dynamic walker locomotion is innately variable due to the non-deterministic nature of ground contact dynamics [3]. This can be accounted to uncontrollable factors including the coefficients of friction and restitution across the walking surface [4]. This can have a major effect on the long-term system dynamics, with each step perturbating the walking gait and impact force, leading to long term instability. A number of proposals have aimed to address this problem. *Byl and Tedrake* suggested that high gain feedback is not able to counter these perturbations, so suggested incorporating the stochastic dynamics of walking in the controller design by employing mean first passage times [5].

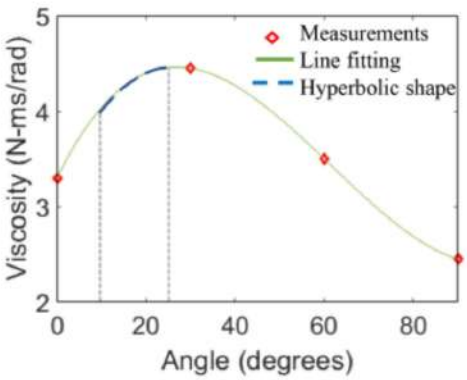

Fig. 1: The damping profile of the knee joint against the knee joint angle. This diagram is taken from *E. Hamid et al's* A state dependent damping method to reduce collision force and its variability' [8].

Biology may offer a more basic solution to this problem. Experiments have shown that the angle-dependent damping profile of the knee joint reduces walking step collision forces and their variability [6]. This damping profile is shown in Figure 1 and was documented by *El Hamid et al*. Experiments have shown that including this same damping profile in robotic systems could improve the stability of their locomotion. *Abdal et al*'s experiment found that incorporating it into an active robotic joint reduced the magnitude and variability of the collision force by 26% and 47% respectively. BLUE is a bipedal robot that has been used to test a variable damper (designed using motor brakes), that was also informed by human biophysics [7], with the purpose of maintaining joints at high stiffness without needing excessive amounts of energy [8].

This paper investigates integrating the angle-dependent damping profile of the knee joint to improve passive dynamic

*This work was supported by a Excellence in Teaching Innovation grant from Imperial College London.

[1]S. Kabir Knupp and Patrick D. McGuckian are with the Dyson School of Design Engineering, Imperial College London, London, SW7 2AZ (emails: kabir.knupp18@imperial.ac.uk, patrick.mcguckian18@imperial.ac.uk)

[2]N. Thrishantha Nanayakkara are with Dyson School of Design Engineering, Imperial College London, London, SW7 2AZ (emails: t.nanayakkara@imperial.ac.uk, u.perera@imperial.ac.uk)

locomotion using the novel fiction based mechanism detailed in Figure 4. The research question is whether the mechanism will reduce the variability of its walking gait and impact force. The damper design could have applications outside of passive dynamics, including reducing the computational load of active locomotion systems or improving the stability of prosthetics.

This paper begins with an explanation of the design of a passive dynamic walker with a variable damping mechanism designed to mimic the human knee's damping characteristics. It then details an experiment aiming to test the mechanism's effect on locomotion and concludes with an analysis and discussion of the experiment's results.

II. Experiment Design

Despite having the potential for multiple use cases, the mechanism was tested on a 'toddler' style passive dynamic walker, the machine that can most simply capture 3D dynamic walking [9]. Testing the damper on this simple gravity-powered walker gives confidence that any measured change in walking results from the inclusion of the damping system.

A. Building the Passive Dynamic Walker

An iterative approach was taken to developing a reliable walker - trialling several different feet geometries and weight distributions to achieve reliable locomotion. The model was intentionally kept small to reduce the time taken to iterate the design and simplify the experimental test rig. 3D computer-aided design software (SolidWorks 2020 and Fusion 360) and 3D printing were used to design and build parts - assuring repeatable designs. This allowed for intricate designs to be trialled, giving more creative freedom when designing the damper.

B. Tuning Physical Parameters

Developing the robot highlighted the key parameters that affected the walker's locomotion. Initial designs failed to walk as they had an exaggerated CAM profile parallel to the walking direction, but only a slight perpendicular profile. This meant the machine fell forwards before beginning to walk. The perpendicular CAM profile is key to achieving the compass gait, as it allows the robot to tilt to one side, lifting the opposing leg off the ground to allow it to swing forward.

Achieving the correct ratio of parallel to perpendicular foot CAM profile is vital for reliable locomotion. However, equally as important is the weight distribution. The weight at the robot's 'head' needs to be sufficient to encourage the robot to tilt sideways and lift one leg of the ground, but if too excessive it won't be able to rock onto the other foot between steps. Furthermore, the feet need to be light enough to be lifted off the ground by the pendulum of the weighted head section, but heavy enough to quickly swing forwards when lifted.

Slots were designed into the robot to allow for the weight to be adjusted in these 3 key areas. The 'head' of the robot was an extruded pentagonal shape with cutouts to press disk weights in each face, creating an even distribution. The inside of each leg was hollow, meaning magnets could be stacked inside. This approach allowed for the mass of each foot to be finely tuned. Caution was taken to make sure there was no interaction between the magnets in each leg.

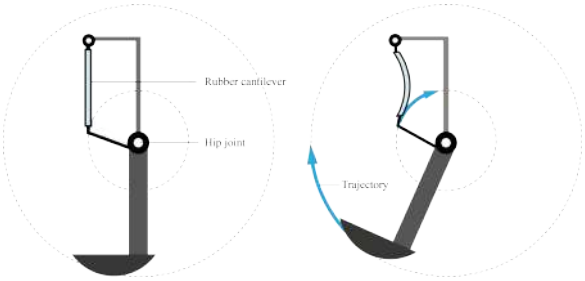

Fig. 2: Preliminary design for a joint angle dependent damper, based off the compression of a rubber cantilever.

By increasing the weight at the top of the robot, the average step size of its locomotion could be increased. This is because the higher weight increased the robot's inertia as it rocked, increasing the period of perpendicular motion. This increased the amount of time each leg was off the ground - allowing it to swing further.

It was also noted that the friction of the surface the robot was walking on significantly affected the stability of its locomotion. The cause of this is explained by *Nanayakkara et al*'s experiments [4]. The robot walked best on a surface with a high amount of friction, thus all experiments were run with the robot walking on 120grit sandpaper.

C. Initial Damping Mechanism

The knee joint's peak viscosity occurs at 25 degrees [10]. Given the expectation is that joint angle will never reach this value, the region of interest is 0-25 degrees. In this region, the damping profile can be simplified to the first quarter of a Sin wave.

Initial designs involved placing the damper at the hip joint and would have theoretically worked by compressing an object (such as a rubber cantilever) as the leg stepped forward. The concept leveraged the changing force components at different leg swing angles that arise from the trajectory of the moving part (see Figure 2) to create a sinusoidal damping mechanism.

This design had a number of limitations. The aim was to dampen the step impact force, however, this mechanism would also dampen the leg's swing. Furthermore, it required the centre 'head' component to be perfectly upright to achieve the intended results.

D. Revised Damping Design

Given the difficulty of mounting the damper to the 'head' of the robot, the decision was made to integrate it into the foot. The revised design splits the foot into front and back pieces and connects them together using two springs - allowing them to slide past each other. As the foot collides with the ground the two sections slide against each other, and the friction works to dampen the impact.

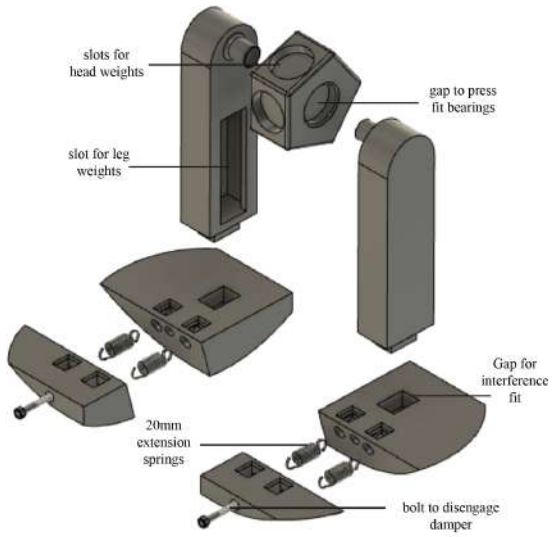

Fig. 3: Exploded view of passive dynamic walker with the embedded friction damper in the feet.

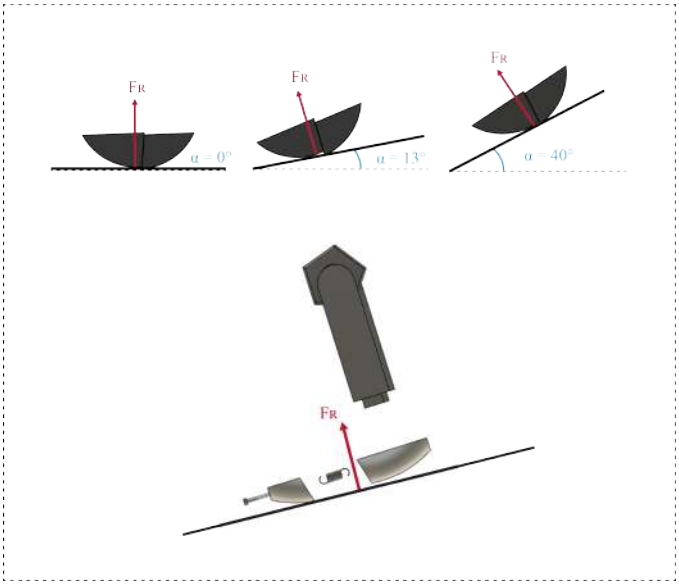

Fig. 4: A visual explanation of the friction damper, where α is the angle of the slope, and F_R is the reaction force (assumed to be normal to the walking surface). There should be more movement and therefore more friction between the split foot components at about $15°$.

The level of frictional resistance is dependent on the angle at which the foot collides with the surface. The closer the ground reaction force is to being parallel to the sliding surfaces, the more energy is released through friction. Furthermore, by varying the angle between the two sections, the angle of peak damping can be controlled. Springs return the mechanism to the resting position as the foot is lifted back up off the ground surface on the next step (see Figure 4).

E. Final Passive Dynamic Walker Design

The final walker, with an embedded disengageable damping mechanism, is shown in Figure 3.

It was 3D printed from 1.75mm PLA filament, and consisted of 7 components: a head, two leg parts that were interference fitted into the rear feet, and two front foot parts. A total of 50g of weight was added to the head component by evenly distributing 5 10g weights. The legs were attached to the head using two 9mm bearings that were press-fit into the headpiece, creating a pin joint. A total of 18g of weight was placed in each leg by stacking 10 neodymium magnets in a cavity. The split in the foot is at an angle of $15°$. The two feet sections were attached to each other using 2 20x5x5.1 mm extension springs in each foot - and 4 M3 threaded inserts were melted into the feet, which allowed a 25mm M3 bolt to fix the separate front and rear feet parts together to lock the mechanism. The final assembly was 13.8cm tall, 13.5cm wide, and had a mass of 174.1g.

F. Ramp Design

A pressure-sensitive ramp was built to measure impact forces as the robot walked. Initial designs used 5mm acrylic, however, this had poor rigidity, meaning as the robot walked, the flexing surface affected its gait. Therefore, 15mm thick

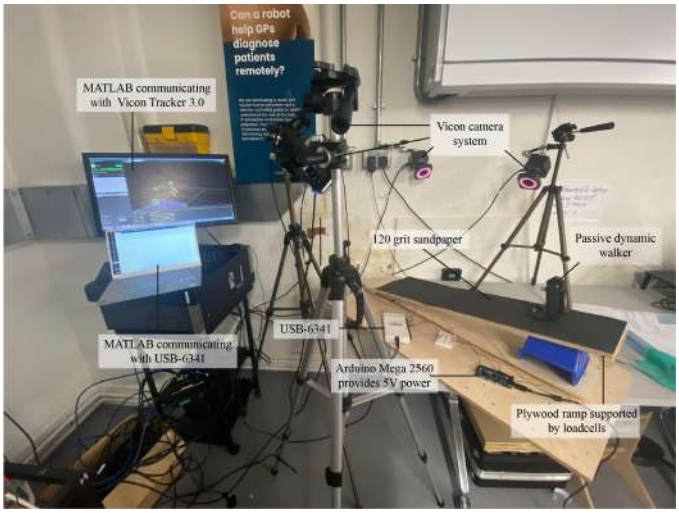

Fig. 5: Experimental setup - This is the test bed that was used for the experiment.

plywood with a 90cm slope was used. The ramp's angle was measured at 9.2 degrees. Initially, it was mounted on four 1kg load cells, and impact forces were to be found by summing their values. This could also be used to track the position of the walker on the ramp, but the use of the Vicon tracking system made this redundant. Due to equipment failure, only 2 pressure cells were used, one at the start and one at the end of the ramp.

G. Technical Set-Up

To collect impact force data as the robot walked over the ramp, a National Instruments USB-6341 was used to import

live data into MATLAB 2021. The load-cells operated on the 5V supply of an Arduino Mega 2560. Once imported, the time-series data from the two DIYmalls 2kg load cells were summed together to get the total force exerted by the walker on the ramp. Force data was sampled at a rate of 37.8Hz, and measurements had an accuracy of 0.05%.

To obtain data for the walker's step angles a Vicon camera tracking system was used. The setup consisted of 4 Vicon Bonita cameras and 1 Vicon Vero camera. The data was sampled at a rate of 200Hz, and measurements had an accuracy of $63 \pm 5\mu m$ and overall precision of 15 μm.

Vicon requires at least 3 points to create and track an object - therefore 3 reflective markers were placed on each leg to create 2 objects. One was placed at the foot, the other at the ankle, and a final at the hip joint (shown in Figure 6). Each marker needed to be visible by at least 3 cameras to derive its position. Given that the walker's geometry can hide the points, the 5 cameras were positioned in a fan motif end of the ramp (see Figure 5). The Vicon system returned the X, Y, and Z positions of each of the 6 points.

The position of the markers in 3D space could be converted into a gait angle by creating two vectors for each of the walkers legs (see Figure 6).

- $H1$=position of the marker at the hip on the left leg
- $A1$=position of the marker at the ankle on the left leg
- $F1$=position of the marker at the foot on the left leg
- $H2$=position of the marker at the hip on the right leg
- $A2$=position of the marker at the ankle on the right leg
- $F2$=position of the marker at the foot on the right leg
- θ=angle between two vectors drawn parallel to each leg
- α= the joint angle being calculated

When calculating the joint angle, foot marker positions can be disregarded. For each set of position data, the following calculation was performed:

$$\overrightarrow{H1A1} = \begin{bmatrix} A1_x - H1_x \\ A1_y - H1_y \\ A1_z - H1_z \end{bmatrix} \quad \overrightarrow{H2A2} = \begin{bmatrix} A2_x - H2_x \\ A2_y - H2_y \\ A2_z - H2_z \end{bmatrix}$$

$$\theta = \arccos\left(\frac{\overrightarrow{H1A1} \cdot \overrightarrow{H2A2}}{\sqrt{\overrightarrow{H1A1}_x^2 + \overrightarrow{H1A1}_y^2 + \overrightarrow{H1A1}_z^2}\sqrt{\overrightarrow{H2A2}_x^2 + \overrightarrow{H2A2}_y^2 + \overrightarrow{H2A2}_z^2}}\right)$$

$$\alpha = \theta - 73^\circ$$

After this, any DC offset was removed, resulting in cleaned step angle data.

The walker's speed was calculated for each trial by dividing the magnitude of the vector $H1_{t2}H1_{t1}$ by $t2-t1$, where $t1$ is the time when the walker is released, and $t2$ is the time the trial is stopped. $H1_{t2}H1_{t1}$ is the distance between the hip marker at time $t1$ - $t2$.

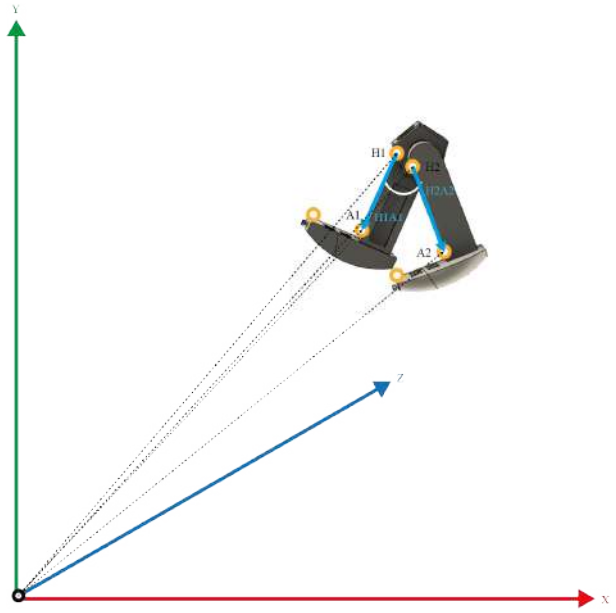

Fig. 6: A representation of the walker in the virtual 3D space created by the Vicon - the orange circles represent the points that were tracked by the Vicon system and the two leg vectors are in blue. The angle between them (illustrated in white) is the leg step angle.

H. Control measures

The experiment measured the variability of the robots gait and impact force with and without the damper. Therefore, for valid results, the physical aspects of the setup were controlled so that any change in behaviour resulted solely from the damper being engaged. Therefore, the following measures were made:

- The passive walker is entirely symmetrical in geometry and weight when reflected in the sagittal plane
- The same robot was used to test with and without damping through the inclusion of a mechanism lock.
- The weights were evenly distributed.
- The wood used for the ramp was consistent in thickness to reduce variation in the coefficient of restitution which leads to walking variation [4].
- Sheets of 120GM sandpaper were adhered to the ramp to reduce variation in the coefficient of friction which leads to walking variation [4].
- The angle of the ramp was identical for all tests.
- The walker was started at the same position on the ramp.

I. Method

The process of the experiment was as follows:

1) The walker was placed at the fixed starting point at the top of the ramp.
2) The walker was rocked to one side and released.
3) The walker made its way to the bottom of the ramp.
4) The Vicon system recorded the positional information needed to derive the walker's leg angles, and the ramp

collected impact force data.

This process was repeated 20 times with the damping mechanism disengaged and 20 times with the damper engaged. Manually releasing the walker created some variation in starting conditions, however, given its locomotion is innately stochastic, after completing the first few steps any effects of this is lost. Nonetheless, an effort was made to keep it consistent.

With the Vicon cameras and pressure-sensitive ramp, the walker's gait angle and impact force of collisions could be calculated. These data points were collected on two separate computers recording data at different frequencies ($200Hz$ for the Vicon and $37.8Hz$ for the USB-6341). However, given peak gait angle occurs at the same point as peak impact force they could be synchronised by passing the time series data through a peak detection algorithm and syncing the time between peaks. Data recording began before the robot started walking, so to remove this excess, a moving variance filter was passed over the signal and the entries where the variance was below a set threshold were discarded.

III. Results

By plotting the time series values for impact force (Figure 7) and walking gait angle (Figure 8) with and without the damper, a clear reduction in variability can be observed - with the damped runs appearing to have a more consistent amplitude and frequency. This can be quantified by calculating the variance (see Table I). On average, the damped walker had a 23.9% lower variance in impact force and an 88.0% lower variance in walking gait angle compared to the undamped walker.

	Collision force		Leg angles	
Run	Undamped	Damped	Undamped	Damped
1	8.29	5.64	5.65	0.15
2	5.87	5.74	3.71	1.15
3	6.66	8.47	4.02	0.71
4	7.23	6.35	2.89	1.15
5	6.79	6.23	5.20	0.67
6	6.27	7.82	3.53	1.32
7	5.35	8.19	5.79	0.83
8	9.56	5.90	12.38	0.90
9	7.55	5.89	5.79	1.57
10	7.93	7.01	10.01	1.23
11	10.36	6.46	10.14	1.04
12	8.70	6.66	6.01	0.93
13	9.02	5.41	7.93	0.77
14	10.35	6.40	9.35	2.01
15	11.59	6.66	11.87	0.70
16	10.58	6.79	9.85	0.70
17	9.23	7.44	7.42	0.71
18	9.03	6.48	11.38	0.60
19	8.67	7.60	11.87	0.67
20	9.54	9.03	7.69	0.59
Average	8.42	6.81	7.72	0.93

TABLE I: Table showing the total variance for each run (the first two columns show the variance in force, and the second two show the variance in leg angles for each step taken)

The impact force data proved to be extremely noisy, thus, even with smoothing, it wasn't suitable for in-depth analysis. Therefore, the rest of the results will only consider gait angle.

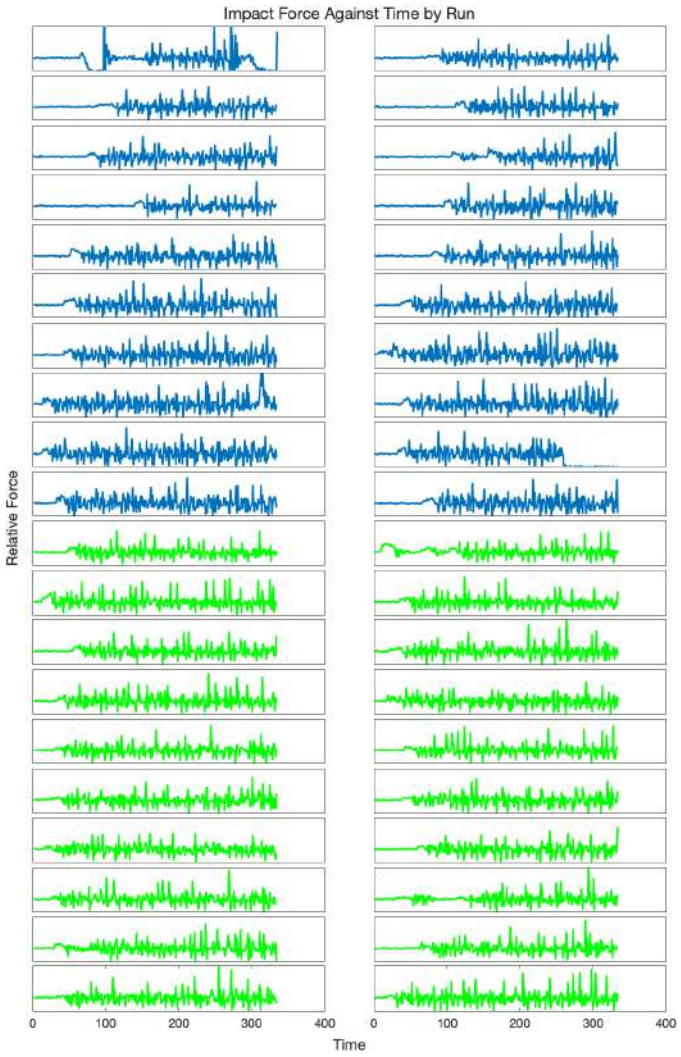

Fig. 7: Raw force data for the passive dynamic walker. The blue graphs display leg angles for undamped walking, and the green graphs show damped walking.

This analysis can be expanded by examining the runs in the frequency domain (see Figure 9). The undamped runs typically show multiple frequency peaks, suggesting that the robot was walking at different frequencies throughout the run. In contrast, the damped values typically show one frequency peak at around 2Hz showing that the gait was consistent.

This raw data analysis proves the validity of the mechanism. However, a better understanding of its impact can be achieved by comparing specific steps between runs. A step occurs at the peak gait angle, so, a peak detection algorithm was used to collect sets of angles for each sequential step (i.e., a set of angles for the first step, a set for the second step etc.). All runs that had gaps in angle data before the 20th step were removed, leaving 16 undamped runs, and 19 damped runs. By averaging the variance of all these sets of steps, it can demonstrated that the damper reduces inter-run step angle variance by 88.7% (0.50 to 4.46). However, this improvement isn't consistent throughout the run.

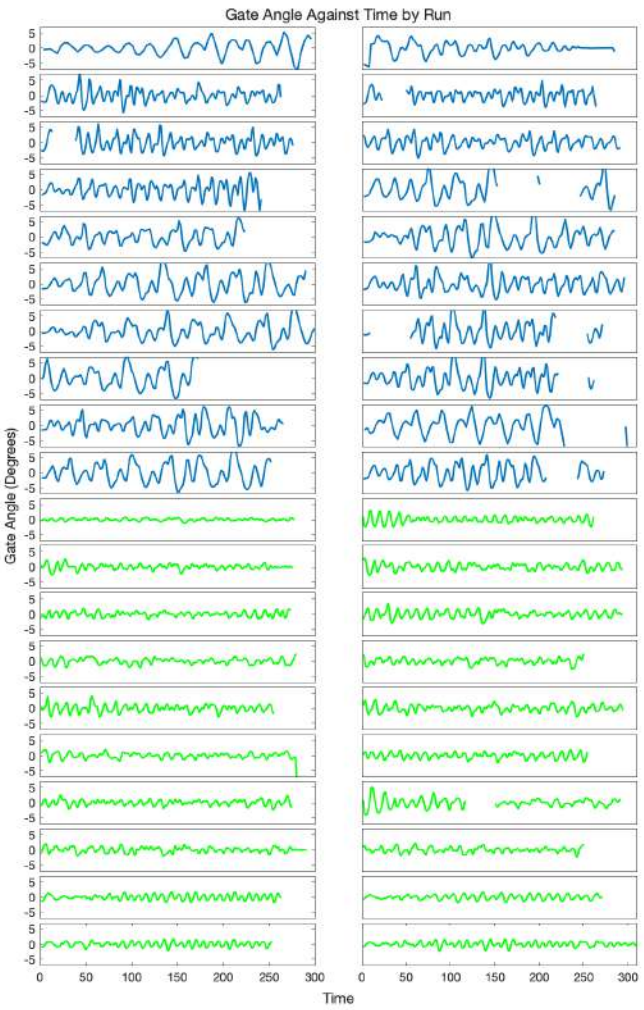

Fig. 8: Raw leg angle data for the passive dynamic walker. The blue graphs display leg angles for undamped walking, and the green graphs show damped walking

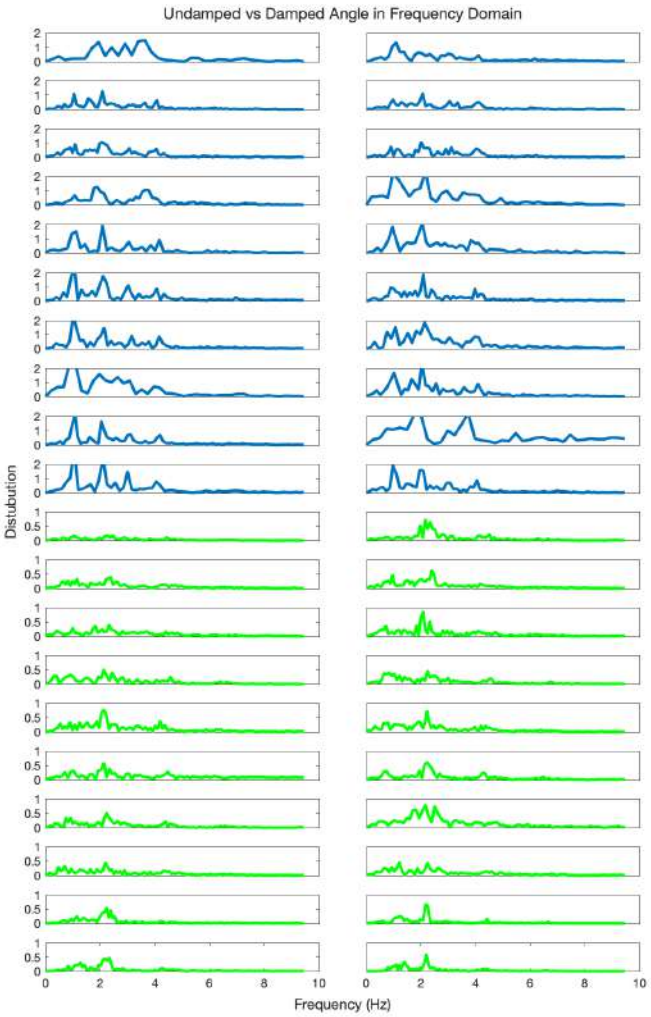

Fig. 9: Fourier series comparison of the undamped walker's leg angles (blue), and damped walker's leg angles (green).

Figure 10 show's the distribution of angles for each step. The damped steps have a tight and consistent distribution throughout the walk. By comparison, the undamped step distributions appear to get wider with each step, suggesting that consistency is dropping throughout locomotion,

The dropping consistency of the undamped walker can be explained by each step's impact changing the robot's dynamics. As it continues to walk these changes compound, leading to increased variability in step angle. The damping mechanism absorbs some of this impact force, thus reducing its effect on the robot's dynamics - keeping the step angles consistent. This is highlighted by plotting the angle variance for each step sequentially (see Figure 11).

One issue with this method of analysis is, when the damper was engaged, the robot took much shorter steps - with the average step angle dropping from 3.26 degrees to 1.10 degrees. This means that the 20th damped step occurred before the 20th undamped step - making comparison difficult. However, the results show that the step variance trends upwards for the undamped walker and downwards for the damped walker - suggesting that this effect will only increase throughout locomotion.

The likelihood of these trends continuing can be explored by plotting Poincaré maps of each trial (see Figure 12). These are return maps of step angles and plot $peak_K$ against $peak_{K+1}$ - indicating gait consistency and how the limit cycle converges throughout locomotion. The undamped plots are inconsistent and stochastic, whereas the damped plots converge to a central point. Convergence implies that the walker has settled into a consistent gait, and stochasticity suggests that the limit cycles are amplified. These plots support the trends seen in Figure 11 and give confidence that they will continue long term.

This deeper analysis suggests that the reduction in variance can be accounted to the mechanism facilitating the robot to settle into a constant gait.

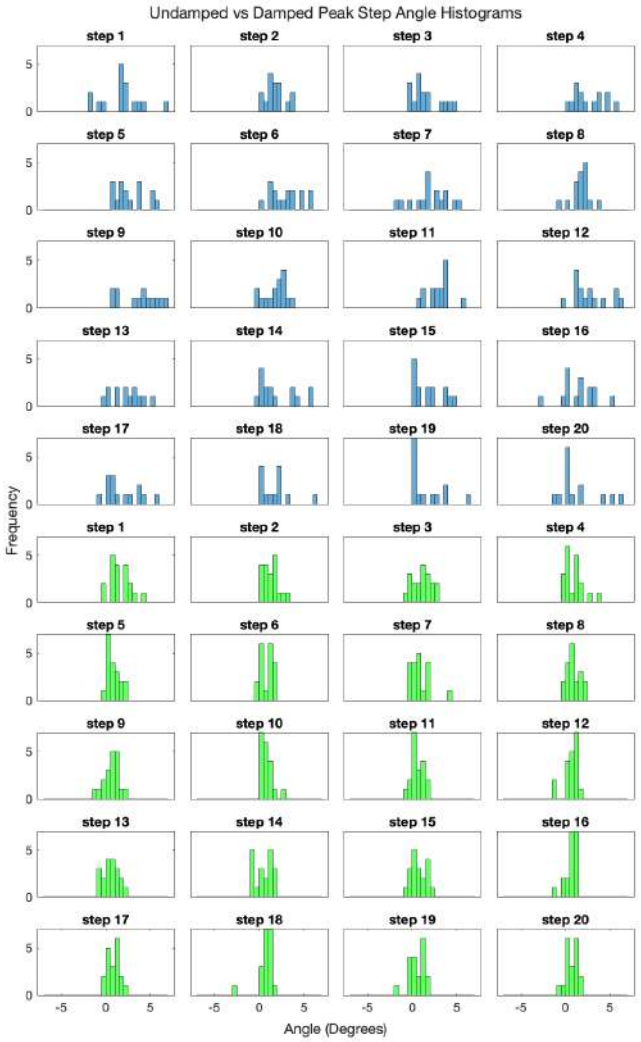

Fig. 10: distribution of leg angles for each step (blue is for the undamped walker, green is for the damped walker)..

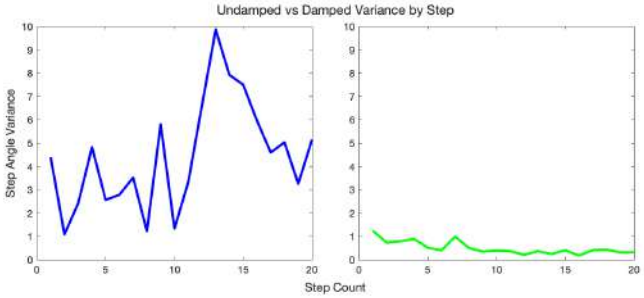

Fig. 11: Variance for each step, up to 20 steps (blue is for the undamped walker, green is for the damped walker).

IV. Discussion

The analysis clearly shows that the inclusion of the proposed damping mechanism can significantly reduce the variation of bipedal locomotion. However, upon reflection, the experiment had several limitations.

Firstly, the noise of the force data meant that peaks

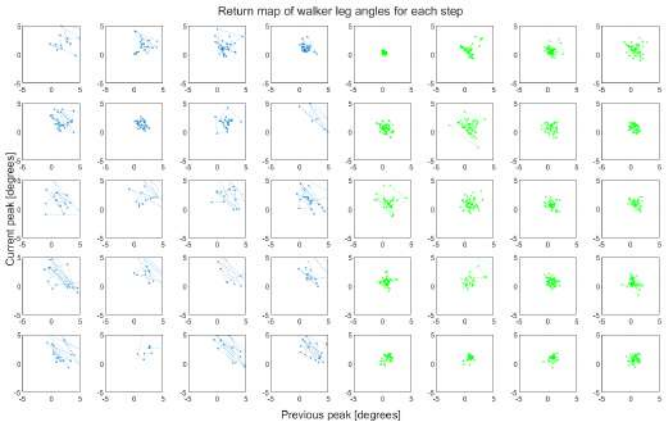

Fig. 12: Poincaré maps for each of the 20 undamped trials (plots in blue), and 20 damped trials (plots in green).

couldn't be identified, even with smoothing. Therefore the results couldn't be verified with a second data source. However, angle data is the more important metric of locomotion stability and is highly correlated with impact force. Nonetheless, the recommendation is this experiment should be repeated with an improved method of force measurement.

Furthermore, one key difference between the damped and undamped runs was a reduction in the overall speed of locomotion. The Vicon data found that the damped walker travelled on average 27% slower than the undamped walker. Given that slower locomotion is inherently more stable, this was likely a factor in the benefits seen. However, while overall speed was lower, step frequency was 8% higher. Given that locomotive variability results from step collision forces, the higher number of steps should lead to a higher variability. The balance of these factors is difficult to determine, and designing an experiment to detangle them would be difficult.

Finally, the sliding damper section was placed far forward on the walker's foot, meaning if the walker took particularly large steps it may land on the heal section of the foot, and thus the damper will have no impact. This means there was a chance that some steps weren't damped. However, the damper was designed to engage at any step angle less than 5 degrees. Given the average angle for damped runs was only 0.9 degrees, it's unlikely this impacted results.

Furthermore, through the analysis of the results, a number of potential future improvements have been identified. The first would be to increase the size of the tracking area of the Vicon camera system allowing for more then the first 20 steps to be analysed. This would give greater confidence in the trends uncovered. Additionally, only one level of damping was tested. There is likely an optimal level of damping for this system - thus future experimentation should explore this.

V. Conclusion

Despite these challenges, the magnitude of the reduction in variability means we can be confident that the damping mechanism proposed in Section II-D could significantly improve locomotion stability. As discussed in the introduction,

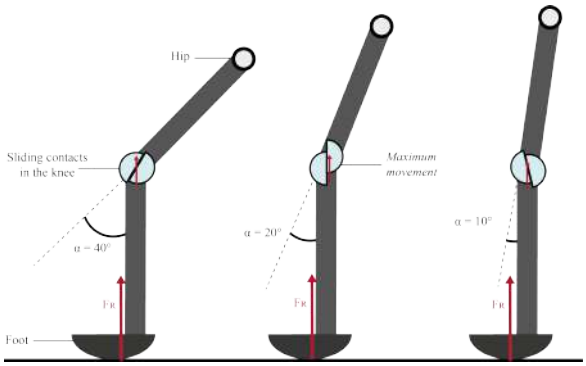

Fig. 13: Diagram depicting how the designed damping mechanism could be included in an artificial knee, where α is the knee joint angle

this mechanism could be applied to active walking systems and prostheses. Furthermore, the integration of the design isn't limited to the foot, Figure 13 details how the same mechanism could be applied to a knee joint. However, all these potential applications are untested, and further experimentation would be required to understand their feasibility.

Taking part in the Robotic Research Project has been a very rewarding experience, and we are delighted to see that our mechanism design has the potential to improve robotic locomotion systems. Given we are both looking towards enrolling in PhD programs for the 2022-2023 academic year, having been able to practice formulating a concise research question, designing experiments to test it in a lab environment and making conclusions using data analysis, has been a valuable experience.

Furthermore, the process has highlighted the value of testing a hypothesis with the most simple experiment possible. By proving testing our mechanism on a passive dynamic toddler, we can be extremely confident in the results as they are few factors that could affect the data. Given the phenomena has been demonstrated in this simple setup we can be confident it can extend to more complex robotic systems. Going forward we will try to replicate the first principles approach we successfully demonstrated in this project.

REFERENCES

[1] S. Collins, A. Ruina, R. Tedrake, and M. Wisse, "Efficient bipedal robots based on passive-dynamic walkers," *Science*, vol. 307, no. 5712, pp. 1082–1085, 2005.

[2] T. McGeer *et al.*, "Passive dynamic walking," *Int. J. Robotics Res.*, vol. 9, no. 2, pp. 62–82, 1990.

[3] M. Garcia, A. Chatterjee, A. Ruina, and M. Coleman, "The simplest walking model: stability, complexity, and scaling," 1998.

[4] T. Nanayakkara, K. Byl, H. Liu, X. Song, and T. Villabona, "Dominant sources of variability in passive walking," in *2012 IEEE International Conference on Robotics and Automation*. IEEE, 2012, pp. 1003–1010.

[5] K. Byl and R. Tedrake, "Metastable walking machines," *The International Journal of Robotics Research*, vol. 28, no. 8, pp. 1040–1064, 2009.

[6] J. W. Smith, J. C. Christensen, R. L. Marcus, and P. C. LaStayo, "Muscle force and movement variability before and after total knee arthroplasty: A review," *World journal of orthopedics*, vol. 5, no. 2, p. 69, 2014.

[7] A. Enoch, A. Sutas, S. Nakaoka, and S. Vijayakumar, "Blue: A bipedal robot with variable stiffness and damping," in *2012 12th IEEE-RAS international conference on humanoid robots (Humanoids 2012)*. IEEE, 2012, pp. 487–494.

[8] E. Hamid, N. Herzig, S.-A. Abad, and T. Nanayakkara, "A state-dependent damping method to reduce collision force and its variability," *IEEE Robotics and Automation Letters*, vol. 6, no. 2, pp. 3025–3032, 2021.

[9] R. Tedrake, T. W. Zhang, M.-f. Fong, and H. S. Seung, "Actuating a simple 3d passive dynamic walker," in *IEEE International Conference on Robotics and Automation, 2004. Proceedings. ICRA'04. 2004*, vol. 5. IEEE, 2004, pp. 4656–4661.

[10] L.-Q. Zhang, G. Nuber, J. Butler, M. Bowen, and W. Z. Rymer, "In vivo human knee joint dynamic properties as functions of muscle contraction and joint position," *Journal of biomechanics*, vol. 31, no. 1, pp. 71–76, 1997.